Energy levels of ^{251}Cf populated in the α decay of $^{255}_{100}$Fm and EC decay of $^{251}_{99}$Es

I. Ahmad,* J. P. Greene, E. F. Moore, F. G. Kondev, and R. R. Chasman
Argonne National Laboratory, Argonne, Illinois 60439, USA

C. E. Porter and L. K. Felker
Nuclear Science and Technology Division, Oak Ridge National Laboratory, Oak Ridge, Tennessee 37831, USA
(Received 10 June 2005; published 16 November 2005)

Gamma-ray singles spectra of extremely pure (chemically and isotopically) samples of ^{255}Fm, with strengths of ~1 mCi, have been measured with a high-resolution 2-cm^2 × 10-mm germanium LEPS detector and with a 25% Ge spectrometer. Gamma rays with intensities as low as 1.0×10^{-6}% per ^{255}Fm α decay have been identified. The electron spectrum of a mass-separated ^{251}Es source was measured with a cooled Si(Li) electron spectrometer. The spectrum provided the conversion coefficients of low-energy transitions in ^{251}Cf and thereby their multipolarities. The present measurements confirm the previous assignments of single-particle states in ^{251}Cf. These include $1/2^+[620]$, 0.0 keV; $7/2^+[613]$, 106.30 keV; $3/2^+[622]$, 177.59 keV; $11/2^-[725]$, 370.47 keV; $9/2^-[734]$, 433.91 keV; $5/2^+[622]$, 543.98 keV; $1/2^-[750]$, 632.0 keV; $9/2^+[615]$, 683 keV; and $9/2^+[604]$, 974.0 keV. A vibrational band was identified in previous studies at 981.4 keV and given an assignment of $\{7/2^+[613] \otimes 2^-\}3/2^-$. Three new vibrational bands are identified in the present work at 942.5, 1086.5, and 1250.0 keV with tentative assignments $\{7/2^+[613] \otimes 1^-\}5/2^-$, $\{7/2^+[613] \otimes 1^-\}9/2^-$, and $\{7/2^+[613] \otimes 0^+\}7/2^+$, respectively. A level was identified at 1185.5 keV with spin of 5/2 or 7/2 but it was not given any configuration assignment. Another level was identified at 1077.5 keV and given a spin of 9/2. Again, no configuration could be assigned to this level.

DOI: 10.1103/PhysRevC.72.054308 PACS number(s): 21.10.Pc, 23.20.−g, 27.90.+b, 25.85.Ca

I. INTRODUCTION

Single-particle energy level spacings in the heaviest nuclei are needed to understand the structure and properties of newly discovered superheavy nuclides and to test theoretical predictions of their stability. The nuclide with the largest odd number of neutrons produced in sufficient quantity for detailed spectroscopy is ^{255}Fm ($t_{1/2} = 20.07$ h). Its decay scheme has been extensively studied by γ-ray and conversion electron spectroscopy [1] and by high-resolution α spectroscopy [2]. The level structure of ^{251}Cf was also studied by the ^{250}Cf(d, p) reaction by using a high-resolution magnetic spectrometer [3]. On the basis of the results of these measurements, neutron single-particle orbitals $1/2^+[620]$, $7/2^+[613]$, $3/2^+[622]$, $5/2^+[622]$, $11/2^-[725]$, $9/2^-[734]$, $1/2^-[750]$, and $9/2^+[615]$ were identified in ^{251}Cf. Recently, ^{255}Fm sources with millicurie strength were used to identify high-lying states in ^{251}Cf. Gamma-singles spectra were measured with a high-resolution Ge spectrometer, and γ-γ coincidence spectra were measured with GAMMASPHERE. These studies [4] determined the excitation energies of the $9/2^+[604]$, $\{7/2^+[613] \otimes 0^+\}7/2^+$, and $\{7/2^+[613] \otimes 2^-\}3/2^-$ states.

Three ^{255}Fm samples were used in the experiments discussed in Ref. [4]. They were produced in the 1998 irradiation cycle at Oak Ridge National Laboratory. These samples contained appreciable amounts of ^{254}Es ($t_{1/2} = 275.7$ d), whose daughter ^{250}Bk ($t_{1/2} = 3.217$ h) produces high-energy γ rays. Compton-scattered photons from these γ rays increased the background below ~800 keV. These samples were placed in a glass bottle or on a quartz disk. Intense α particles from ^{255}Fm produced high-energy γ rays by (α, $p\gamma$) reactions on light elements, which also increased the background. Both of these effects reduced the sensitivity of our earlier measurement. For the experiments reported in this article, extremely pure ^{255}Fm samples, either on quartz or Pt disks, were used. These samples were used to determine γ-ray energies and intensities accurately.

The electron capture decay of ^{251}Es ($t_{1/2} = 33$ h) was studied [5] by measuring its γ-ray spectrum with a Ge(Li) spectrometer. In the present work, we report the measurement of a ^{251}Es conversion electron spectrum with a cooled Si(Li) detector. The present studies of ^{255}Fm γ rays and ^{251}Es electron lines confirm previous assignments of single-particle states and provide information on several new vibrational states.

II. EXPERIMENTAL METHODS AND RESULTS: γ-RAY AND CONVERSION-ELECTRON SPECTROSCOPY

The nuclide ^{255}Fm, which is the daughter of ^{255}Es ($t_{1/2} =$ 38.3 d), was chemically separated from ~1 mg of Es (isotopic composition 99.5% ^{253}Es, ~0.4% ^{254}Es, ~0.04% ^{255}Es) produced in the high-flux isotope reactor (HFIR) at Oak Ridge National Laboratory. Three chemically purified samples of Fm, ~2 mCi each, were shipped to Argonne National Laboratory in 2000 for γ-ray spectroscopic studies. Two additional samples were obtained in 2003. The samples used in our previous studies [4] were placed either in a glass bottle or on a quartz disk. In the γ-ray spectra of those samples, we observed γ rays produced by the reactions of α particles on ^{14}N, ^{19}F, ^{23}Na, ^{28}Si,

*Electronic address: ahmad@phy.anl.gov

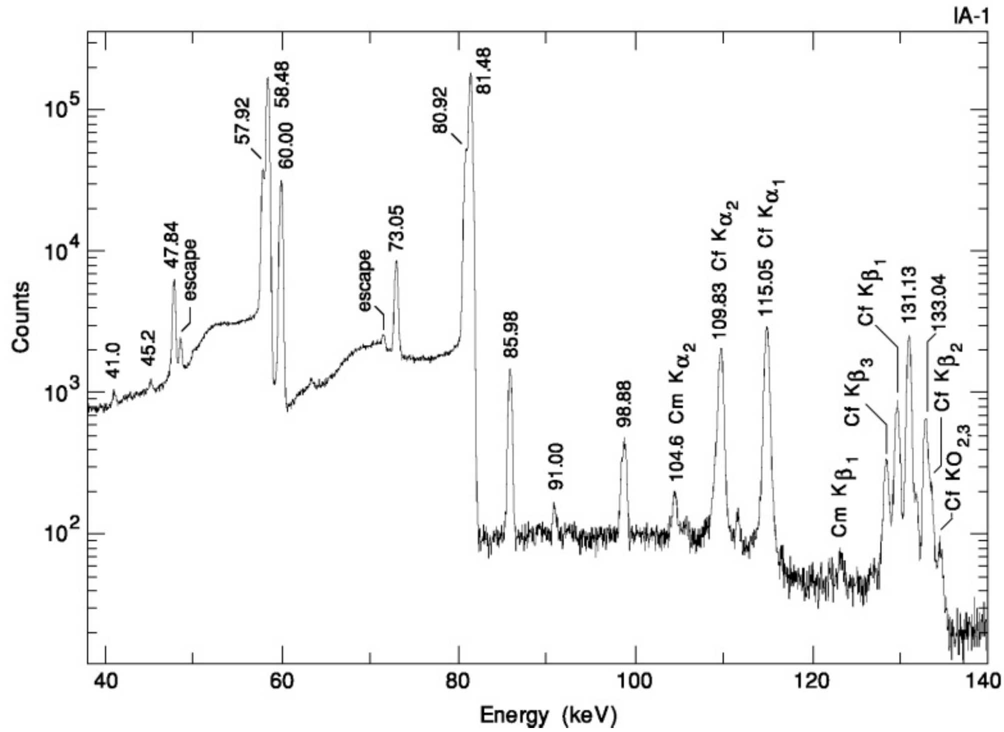

FIG. 1. ^{255}Fm γ-ray spectrum measured with a 2-cm^2 $\times$10-mm LEPS spectrometer through a set of Cu and Al absorbers. The source was sandwiched between two quartz plates, and it was placed 2.5 cm from the detector. The measurement was started 3 d after chemical separation, and the counting time was 17 h.

and ^{35}Cl. These γ rays interfered with ^{255}Fm γ rays, and they also increased the background under the peaks of interest. For this reason, samples used in the present study were sandwiched either between two quartz disks for the measurement of the

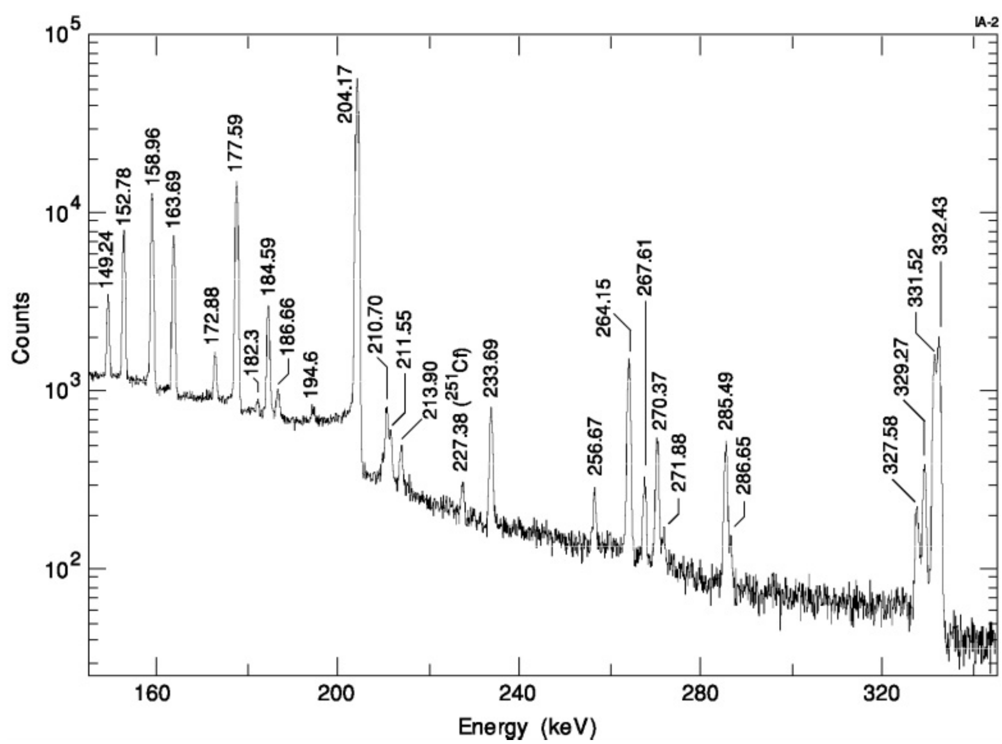

FIG. 2. ^{255}Fm γ-ray spectrum measured with a 2-cm^2 $\times$ 10-mm LEPS spectrometer through a set of Ta, Cd, Cu, and Al absorbers. The source was sandwiched between two 0.5-g/cm^2 Pt disks, and the measurement was started 1 d after chemical separation. Counting time was 20 h.

low-energy γ-ray spectrum or between two Pt disks for the measurement of high-energy γ rays.

The low-energy portion of the γ-ray spectrum of a ^{255}Fm source, sandwiched between two 1-mm quartz disks, measured with a 2-cm$^2\times$10-mm low-energy photon spectrometer (LEPS) is displayed in Fig. 1. A set of Cu and Al absorbers was used to absorb Cf L x rays, thus reducing their summing with γ rays. Gamma-ray spectra of a sample sandwiched between two 0.5 g/cm^2 Pt disks were measured with the LEPS detector and with a 25% Ge spectrometer. High-energy portions of these spectra are displayed in Figs. 2–4. A set of Ta, Cd, Cu, and Al absorbers was used to absorb Cf K x rays and low-energy γ rays, thus reducing the count rate and also reducing summing of γ rays. Energies of γ rays were determined by using internal standards, i.e., by measuring the spectrum of Fm and calibration sources simultaneously. These energies are more accurate than values reported in earlier publications. Gamma-ray intensities were determined by calibrating the detectors with a mixed source containing ^{109}Cd, ^{57}Co, ^{139}Ce, ^{203}Hg, ^{113}Sn, ^{85}Sr, ^{137}Cs, ^{88}Y, and ^{60}Co. ^{255}Fm γ-ray energies and intensities in photons per 100 ^{255}Fm α decays are given in Table I. The intensities are normalized to the intensity of the Cf K_{α_1} x ray (115.05 keV) determined in Ref. [1]. The uncertainties in the table represent uncertainties in the absolute intensities. Uncertainties in the relative intensities are 5% for strong lines.

Gamma-ray lines were assigned to ^{255}Fm α decay on the basis of their decay with the characteristic half-life of ^{255}Fm and the fact that they were present in spectra of different samples with the same relative intensities. Very weak γ rays were assigned to ^{255}Fm α decay because of their fit in the level scheme and the fact that they decayed with a half-life of approximately 1 d. The γ-ray spectra were measured at regular intervals for 1 month. No γ-ray impurity line was observed in these spectra. In addition to the γ rays produced in the α decay of ^{255}Fm, γ rays produced by reactions of ^{255}Fm α particles on light elements and γ rays produced in the ^{255}Fm spontaneous fission also decay with the characteristic half-life of ^{255}Fm. Gamma-ray lines associated with nuclear reactions of α particles with light elements were identified on the basis of their different relative intensities in spectra of samples on different backing materials. The fission branch of ^{255}Fm is listed as 2.4×10^{-5}% [6], and the maximum cumulative yield of any mass number is ~6% [7]. Thus, any γ ray produced in fission will have a maximum intensity of ~1.4×10^{-6}% per ^{255}Fm decay.

The electron spectrum of a mass-separated ^{251}Es sample was measured with a cooled Si(Li) electron spectrometer and is displayed in Fig. 5. The source was the decay product of a mass-separated ^{251}Fm sample used for its decay studies [8]. The detector had a resolution [full width at half-maximum (FWHM)] of 1.0 keV at 100 keV electron energy, and the spectrum was measured at an efficiency-geometry product of 1.0%. The γ-ray spectrum of a ^{251}Es source was also measured with a 25-cm^3 Ge(Li) spectrometer and is included in Fig. 5. Conversion coefficients and multipolarities were determined by using measured γ-ray and electron intensities. Intensities are given in percent per ^{251}Es electron capture decay and were obtained by using measured relative intensities and theoretical

TABLE I. ^{255}Fm γ rays. Singles spectra were measured with a 2-cm$^2\times$10-mm LEPS spectrometer and a 25% Ge detector. Gamma rays not placed in the level scheme are given at the end of the table; c denotes γ rays seen in γ-γ coincidence measurement only.

Energy (keV)	Intensity (% per ^{255}Fm α decay)	Transition Initial (keV) $\rightarrow$Final (keV)
41.0 ± 0.1	$(1.5\pm0.4)\times10^{-3}$	$146.72\rightarrow105.74$
45.2 ± 0.1	$(9\pm2)\times10^{-4}$	$370.47\rightarrow325.33$
47.84 ± 0.02	$(2.5\pm0.3)\times10^{-2}$	$47.84\rightarrow0.0$
57.92 ± 0.03	0.16 ± 0.02	$105.74\rightarrow47.84$
58.48 ± 0.02	0.80 ± 0.06	$106.30\rightarrow47.84$
60.00 ± 0.02	0.14 ± 0.015	$166.30\rightarrow106.30$
63.4 ± 0.1	$(1.0\pm0.3)\times10^{-3}$	$433.91\rightarrow370.47$
73.05 ± 0.02	$(2.8\pm0.3)\times10^{-2}$	$239.35\rightarrow166.30$
80.92 ± 0.05	0.23 ± 0.02	$105.74\rightarrow24.82$
81.48 ± 0.02	1.00 ± 0.08	$106.30\rightarrow24.82$
85.98 ± 0.02	$(7.5\pm0.8)\times10^{-3}$	$325.33\rightarrow239.35$
91.00 ± 0.05	$(3.2\pm0.5)\times10^{-4}$	$237.69\rightarrow146.72$
98.88 ± 0.02	$(2.8\pm0.3)\times10^{-3}$	$146.72\rightarrow47.84$
109.83 ± 0.05	$(1.80\pm0.15)\times10^{-2}$	Cf K_{α_2}
111.78 ± 0.05	$(4.6\pm0.7)\times10^{-4}$	$258.51\rightarrow146.72$
115.05 ± 0.05	$(2.8\pm0.2)\times10^{-2}$	Cf K_{α_1}
128.58 ± 0.05	$(3.3\pm0.3)\times10^{-3}$	Cf K_{β_3}
129.81 ± 0.05	$(8.7\pm0.7)\times10^{-3}$	Cf K_{β_1}
131.13 ± 0.05	$(2.7\pm0.3)\times10^{-2}$	$370.47\rightarrow239.35$
131.95 ± 0.05	$(1.7\pm0.2)\times10^{-3}$	$237.69\rightarrow105.74$
133.04 ± 0.05	$(6.8\pm0.7)\times10^{-3}$	$239.35\rightarrow106.30$
133.73 ± 0.05	$(2.0\pm0.2)\times10^{-3}$	Cf $K_{\beta_2}+K_{\beta_4}$
134.68 ± 0.05	$(7.5\pm0.7)\times10^{-4}$	Cf $K_{O_{2,3}}$
149.24 ± 0.02	$(6.0\pm0.4)\times10^{-4}$	$295.96\rightarrow146.72$
152.78 ± 0.02	$(1.80\pm0.14)\times10^{-3}$	$177.59\rightarrow24.82$ $+258.51\rightarrow105.74$
158.96 ± 0.02	$(4.2\pm0.3)\times10^{-3}$	$325.33\rightarrow166.30$
163.69 ± 0.02	$(2.00\pm0.15)\times10^{-3}$	$211.53\rightarrow47.84$
172.88 ± 0.03	$(2.5\pm0.3)\times10^{-4}$	$319.63\rightarrow146.72$
177.59 ± 0.03	$(4.5\pm0.3)\times10^{-3}$	$177.59\rightarrow0.0$
182.3 ± 0.3	$\sim6\times10^{-5}$	$420.0\rightarrow237.69$?
184.59 ± 0.03	$(8.7\pm0.7)\times10^{-4}$	$423.92\rightarrow239.35$
186.66 ± 0.05	$(1.10\pm0.15)\times10^{-4}$	$211.53\rightarrow24.82$
194.6 ± 0.4	$(3.4\pm0.5)\times10^{-5}$	$433.91\rightarrow239.35$ and 204.1 escape peak
197.4 ± 0.4	$(7\pm2)\times10^{-6}$	$589.98\rightarrow392.39$
204.17 ± 0.02	$(2.40\pm0.18)\times10^{-2}$	$370.47\rightarrow166.30$
209.7 ± 0.2	$\sim5\times10^{-5}$	$535.0\rightarrow325.33$?
210.70 ± 0.04	$(2.8\pm0.4)\times10^{-4}$	$258.51\rightarrow47.84$
211.55 ± 0.05	$(1.3\pm0.2)\times10^{-4}$	$211.53\rightarrow0.0$
213.90 ± 0.05	$(1.18\pm0.12)\times10^{-4}$	$319.63\rightarrow105.74$
233.69 ± 0.02	$(3.5\pm0.25)\times10^{-4}$	$258.51\rightarrow24.82$
245.7 ± 0.4	$(7\pm2)\times10^{-6}$	$392.39\rightarrow146.72$
256.67 ± 0.05	$(8.6\pm0.8)\times10^{-5}$	$648.95\rightarrow392.39$
264.15 ± 0.03	$(1.04\pm0.08)\times10^{-3}$	$370.47\rightarrow106.30$
267.61 ± 0.04	$(1.52\pm0.15)\times10^{-4}$	$433.91\rightarrow166.30$
270.37 ± 0.03	$(3.5\pm0.3)\times10^{-4}$	$589.98\rightarrow319.63$
271.88 ± 0.05	$\sim3\times10^{-5}$	$319.63\rightarrow47.84$
285.49 ± 0.03	$(3.7\pm0.4)\times10^{-4}$	$543.98\rightarrow258.51$
286.65 ± 0.05	$(5.4\pm0.5)\times10^{-5}$	$392.39\rightarrow105.74$
301.0 ± 0.3^{c}	$\sim5\times10^{-7}$	$1009.0\rightarrow708.0$
327.58 ± 0.04	$(2.1\pm0.2)\times10^{-4}$	$433.91\rightarrow106.30$
329.27 ± 0.04	$(4.4\pm0.4)\times10^{-4}$	$648.95\rightarrow319.63$

TABLE I. (*Continued*).

Energy (keV)	Intensity (% per ^{255}Fm α decay)	Transition Initial (keV) → Final (keV)
331.52 ± 0.04	$(1.8 \pm 0.2)\times 10^{-3}$	589.98 → 258.51
332.43 ± 0.04	$(2.5 \pm 0.2)\times 10^{-3}$	543.98 → 211.53
349.6 ± 0.3[c]	$\sim 1\times 10^{-6}$	981.4 → 632.0
350.6 ± 0.2	$(8 \pm 1)\times 10^{-6}$	589.98 → 239.35
366.4 ± 0.1	$(5.7 \pm 0.4)\times 10^{-3}$	543.98 → 177.59
378.5 ± 0.1	$(2.6 \pm 0.19)\times 10^{-3}$	589.98 → 211.53
381.0 ± 0.3[c]	$\sim 2\times 10^{-6}$	981.4 → 600.8
390.4 ± 0.1	$(4.5 \pm 0.3)\times 10^{-4}$	648.95 → 258.51
395.3 ± 0.2	$(7 \pm 1)\times 10^{-6}$	720.5 → 325.33
397.5 ± 0.2	$(2.5 \pm 0.5)\times 10^{-6}$	543.98 → 146.72
400.9 ± 0.2	$(2.9 \pm 0.4)\times 10^{-5}$	720.5 → 319.63
408.2 ± 0.2[c]	$\sim 2\times 10^{-6}$	1009.0 → 600.8
409.6 ± 0.1	$(1.25 \pm 0.12)\times 10^{-4}$	648.95 → 239.35
412.2 ± 0.2	$(3.3 \pm 0.3)\times 10^{-5}$	589.98 → 177.59
423.7 ± 0.1	$(7.1 \pm 0.5)\times 10^{-4}$	589.98 → 166.30
437.7 ± 0.1	$(1.65 \pm 0.12)\times 10^{-3}$	543.98 → 106.30
443.2 ± 0.1	$(6.4 \pm 0.5)\times 10^{-5}$	589.98 → 146.72
454.4 ± 0.3	$\sim 5\times 10^{-7}$	632.0 → 177.59
478.3 ± 0.2	$(8 \pm 1)\times 10^{-7}$	625.3 → 146.72
482.5 ± 0.3	$(5.7 \pm 0.6)\times 10^{-5}$	648.95 → 166.30
483.7 ± 0.2	$(3.6 \pm 0.26)\times 10^{-4}$	589.98 → 106.30
496.2 ± 0.2	$(2.00 \pm 0.15)\times 10^{-4}$	543.98 → 47.84
502.1 ± 0.2	$(7.5 \pm 0.6)\times 10^{-5}$	648.95 → 146.72
519.2 ± 0.2	$(2.2 \pm 0.17)\times 10^{-4}$	543.98 → 24.82
530.4 ± 0.4	$\sim 5\times 10^{-7}$	708.0 → 177.59
542.2 ± 0.2	$(2.8 \pm 0.3)\times 10^{-4}$	589.98 → 47.84
543.9 ± 0.2	$(2.0 \pm 0.2)\times 10^{-4}$	543.98 → 0.0
553.0 ± 0.2	$(3.5 \pm 0.6)\times 10^{-6}$	600.8 → 47.84
565.2 ± 0.2	$(6.5 \pm 0.5)\times 10^{-5}$	589.98 → 24.82
573.7 ± 0.2	$(6.7 \pm 0.6)\times 10^{-6}$	720.5 → 146.72
577.5 ± 0.3	$(3.5 \pm 0.4)\times 10^{-6}$	625.3 → 47.84
		+600.8 → 24.82
601.0 ± 0.2	$(1.70 \pm 0.15)\times 10^{-5}$	648.95 → 47.85
601.0 ± 0.4[c]	$\sim 2\times 10^{-6}$	600.8 → 0.0
607.1 ± 0.4	$(1.3 \pm 0.2)\times 10^{-6}$	632.0 → 24.82
614.5 ± 0.4	$(1.6 \pm 0.2)\times 10^{-6}$	720.5 → 106.30
632.1 ± 0.2	$(2.1 \pm 0.2)\times 10^{-6}$	632.0 → 0.0
641.6 ± 0.3	$\sim 1\times 10^{-6}$	1185.5 → 544.0
643.6 ± 0.3	$\sim 1\times 10^{-6}$	1077.5 → 433.9
652.5 ± 0.2	$(3.6 \pm 0.3)\times 10^{-6}$	1086.5 → 433.91
660.2 ± 0.2	$(5.1 \pm 0.4)\times 10^{-6}$	708.0 → 47.84
683.2 ± 0.3	$(1.5 \pm 0.3)\times 10^{-6}$	708.0 → 24.82
702.3 ± 0.3	$(1.4 \pm 0.3)\times 10^{-6}$	1094.5 → 392.39
707.0 ± 0.3	$(3.0 \pm 0.6)\times 10^{-6}$	1077.5 → 370.47
715.8 ± 0.4	$(2.4 \pm 0.4)\times 10^{-6}$	1086.5 → 370.47
724.1 ± 0.4	$(4.9 \pm 0.5)\times 10^{-6}$	1043.9 → 319.63
731.0 ± 0.2	$(2.8 \pm 0.3)\times 10^{-6}$	942.5 → 211.53
734.5 ± 0.2	$(1.9 \pm 0.2)\times 10^{-6}$	974.0 → 239.35
750.5 ± 0.2	$(4.3 \pm 0.4)\times 10^{-6}$	1009.0 → 258.51
763.5 ± 0.4	$\sim 2\times 10^{-6}$	1155.8 → 392.39
764.7 ± 0.3	$(4.9 \pm 0.5)\times 10^{-6}$	942.5 → 177.59
770.0 ± 0.4	$(8 \pm 1)\times 10^{-6}$	981.4 → 211.53
785.4 ± 0.2	$(9 \pm 1)\times 10^{-7}$	1043.9 → 258.51
797.6 ± 0.2	$(9.4 \pm 0.7)\times 10^{-6}$	1009.0 → 211.53
803.8 ± 0.2	$(1.10 \pm 0.08)\times 10^{-5}$	981.4 → 177.59
807.7 ± 0.2	$(1.10 \pm 0.08)\times 10^{-5}$	974.0 → 166.30

TABLE I. (*Continued*).

Energy (keV)	Intensity (% per ^{255}Fm α decay)	Transition Initial (keV) → Final (keV)
816.1 ± 0.3	$(3.5 \pm 0.4)\times 10^{-6}$	1250.0 → 433.91
831.9 ± 0.2	$(6.0 \pm 0.5)\times 10^{-6}$	1009.0 → 177.59
		+1043.9 → 211.53
836.2 ± 0.2	$(2.8 \pm 0.2)\times 10^{-5}$	942.5 → 106.30
838.4 ± 0.3	$\sim 2\times 10^{-6}$	1077.5 → 239.35
847.0 ± 0.3	$(2.2 \pm 0.3)\times 10^{-6}$	1086.5 → 239.35
859.8 ± 0.3	$(1.8 \pm 0.3)\times 10^{-6}$	1155.8 → 295.96
867.8 ± 0.2	$(1.00 \pm 0.08)\times 10^{-5}$	974.0 → 106.30
903.1 ± 0.3	$(1.4 \pm 0.2)\times 10^{-6}$	1009.0 → 105.74
911.3 ± 0.1	$(1.20 \pm 0.10)\times 10^{-5}$	1077.5 → 166.30
918.1 ± 0.3	$\sim 1.0\times 10^{-6}$	1155.8 → 237.69
920.5 ± 0.3	$(2.1 \pm 0.4)\times 10^{-6}$	1086.5 → 166.30
938.1 ± 0.3	$(1.6 \pm 0.2)\times 10^{-6}$	1043.9 → 105.74
947.8 ± 0.3	$(1.6 \pm 0.2)\times 10^{-6}$	1094.5 → 146.72
956.6 ± 0.2	$(2.9 \pm 0.3)\times 10^{-6}$	981.4 → 24.82
961.2 ± 0.2	$(4.6 \pm 0.4)\times 10^{-6}$	1009.0 → 47.84
971.2 ± 0.1	$(2.9 \pm 0.22)\times 10^{-5}$	1077.5 → 106.30
981.4 ± 0.2	$(1.50 \pm 0.15)\times 10^{-5}$	981.4 → 0.0
984.2 ± 0.2	$(1.10 \pm 0.12)\times 10^{-5}$	1009.0 → 24.82
988.8 ± 0.3	$(3.3 \pm 0.5)\times 10^{-6}$	1094.5 → 105.74
991.6 ± 0.3	$(2.3 \pm 0.4)\times 10^{-6}$	1250.0 → 258.51
996.1 ± 0.2	$(1.10 \pm 0.08)\times 10^{-5}$	1043.9 → 47.84
1019.2 ± 0.3	$(1.0 \pm 0.3)\times 10^{-6}$	1185.5 → 166.30
1038.3 ± 0.3	$(2.2 \pm 0.5)\times 10^{-6}$	1250.0 → 211.53
1072.3 ± 0.3	$(5.0 \pm 0.7)\times 10^{-6}$	1250.0 → 177.59
1079.1 ± 0.3	$(3.8 \pm 0.5)\times 10^{-6}$	1185.5 → 106.30
1083.9 ± 0.3	$(5.5 \pm 0.7)\times 10^{-6}$	1250.0 → 166.30
1144.0 ± 0.4	$\sim 7\times 10^{-7}$	1250.0 → 106.30
404.0 ± 0.3	$(2.0 \pm 0.3)\times 10^{-6}$	unassigned
416.9 ± 0.3	$(3.2 \pm 0.5)\times 10^{-6}$	unassigned
463.2 ± 0.3	$(7.8 \pm 0.9)\times 10^{-6}$	unassigned
556.0 ± 0.3	$(3.8 \pm 0.6)\times 10^{-6}$	unassigned
579.1 ± 0.4	$(1.1 \pm 0.2)\times 10^{-6}$	unassigned
583.0 ± 0.4	$(2.8 \pm 0.3)\times 10^{-6}$	unassigned
637.0 ± 0.3	$(2.0 \pm 0.2)\times 10^{-6}$	unassigned
747.8 ± 0.4	$(8.7 \pm 0.8)\times 10^{-6}$	unassigned
754.6 ± 0.4	$(3.3 \pm 0.3)\times 10^{-6}$	unassigned
774.0 ± 0.2	$(3.8 \pm 0.3)\times 10^{-5}$	unassigned
778.9 ± 0.4	$(5.4 \pm 0.6)\times 10^{-7}$	unassigned
789.2 ± 0.4	$(1.10 \pm 0.14)\times 10^{-6}$	unassigned
794.1 ± 0.4	$(6.7 \pm 0.9)\times 10^{-7}$	unassigned
851.7 ± 0.3	$(5.6 \pm 0.5)\times 10^{-6}$	unassigned
890.8 ± 0.5	$(1.2 \pm 0.4)\times 10^{-6}$	unassigned
900.3 ± 0.4	$(1.2 \pm 0.3)\times 10^{-6}$	unassigned

K/total capture ratios. The results from the analysis of γ-ray and electron spectra are given in Table II. Also included are theoretical conversion coefficients from the most recent calculation [9]. In addition to conversion-electron lines, Cf *K* x-ray peaks and Cf *K*-Auger lines are present in the spectrum. The intensity of Cf *K* x rays, not included in Table II, was deduced to be 64% ± 5% per ^{251}Es EC decay.

In Table II, intensities of 71.5-, 81.2-, and 129.8-keV γ rays are not given because these γ rays were not observed in the γ-ray spectrum owing to their weak intensities and interference

TABLE II. ^{251}Es conversion electron data. The electron spectrum was measured with a cooled Si(Li) spectrometer and the γ-ray spectrum with a 25-cm^3 Ge(Li) detector.

Transition Energy (keV)	Shell	Energy (keV)	Intensity (%)	Conversion Coefficient	Theory	Multipolarity
71.5	$L2$	46.4	~0.25		2.0($M1$), 44($E2$)	$E2$
	$L3$	52.0	~0.20		0.07($M1$), 31($E2$)	
	M	65.8	~0.20		4.2($M1$), 22($E2$)	
	N	70.1	~0.06		1.5($M1$), 8.0($E2$)	
81.2	$L_1 + L_2$	56.1	~0.13		12($M1$), 26($E2$)	$E2$
	M	75.3	~0.06		2.9($M1$), 12($E2$)	
129.8	$L_1 + L_2$	103.8	2.5 ± 0.2		3.0($M1$), 3.2($E2$)	$M1$
	M	123.1	0.62 ± 0.05		0.74($M1$), 1.38($E2$)	
152.8	$L_1 + L_2$	126.9	1.00 ± 0.08	1.9 ± 0.23	1.9($M1$), 1.6($E2$)	$M1$
	M	146.1	0.24 ± 0.02	0.45 ± 0.05	0.46($M1$), 0.66 ($E2$)	
	γ	152.8	0.53 ± 0.045			
163.8	$L_1 + L_2$	137.8	0.09 ± 0.02	1.6 ± 0.3	1.5($M1$), 1.2 ($E2$)	$M1$
	γ	163.7	0.056 ± 0.007			
177.6	K	42.7	6.6 ± 0.55	5.1 ± 0.6	5.8 ($M1$), 0.15 ($E2$)	$M1$+13%$E2$
	$L_1 + L_2$	151.6	1.52 ± 0.13	1.17 ± 0.14	1.22 ($M1$), 0.85 ($E2$)	
	L_3	157.6	0.078 ± 0.015	0.06 ± 0.01	0.0045 ($M1$), 0.35($E2$)	
	M	170.9	0.39 ± 0.033	0.30 ± 0.04	0.30 ($M1$), 0.34($E2$)	
	N	175.8	0.16 ± 0.014	0.12 ± 0.014	0.11 ($M1$), 0.12 ($E2$)	
	γ	177.6	1.30 ± 0.11			

with the strong Cf $K_{\beta_1'}$, peak. The 71.5-keV transition is given $E2$ multipolarity on the basis of the L_2/L_3 ratio, and the 81.2-keV transition has been shown in previous studies to have an $E2$ multipolarity. The 177.6 L_3 peak contains the 163.8 M line. The intensity of the 177.6 L_3 line was obtained after subtracting the intensity of the 163.8 M line deduced from the measured intensity of the 163.8 L_1 line and theoretical conversion coefficients.

The conversion-electron spectrum of a thin ^{255}Fm source was also measured with a 6-mm×6-mm PIN diode with 0.3-mm thickness. The PIN diode was operated at room temperature and had an energy resolution (FWHM) of 2.5 keV. Only conversion lines from the 177.6-, 332.0-, 366.4-, and 378.5-keV transitions were observed, and their intensities gave the multipolarities of all these transitions as $M1$, as was deduced in Ref. [1].

III. DISCUSSION

A. Level scheme

Although high-energy γ-ray transitions were used to deduce the levels reported in [4], the energies and intensities of γ rays above 544 keV are reported here for the first time to our knowledge. In addition, several new lines below 544 keV have been observed. The data used for the single-particle orbital assignments have been discussed in detail in previous publications. Here, we present those arguments in brief with emphasis on new data.

Levels in ^{251}Cf so far identified are displayed in Figs. 6 and 7. Energies of most of the levels were obtained directly from the ^{255}Fm α spectrum [2] and the ^{250}Cf(d, p) reaction spectrum [3]. However, more precise level energies were obtained from the γ-ray energies, and these are given in Figs. 6 and 7. Alpha-gamma coincidence data [1] show γ rays deexciting levels populated in the α decay. Also, multipolarities of most of the low-energy transitions were determined by the measurement of subshell ratios and conversion coefficients [1]. The γ-γ coincidence measurement with GAMMASPHERE, described in Ref. [4], was extremely useful in the identification of several rotational bands.

The ground state of ^{251}Cf is established as $1/2^+[620]$ on the basis of its α decay [10] to ^{247}Cm. Additional confirmation comes from the excellent agreement of the decoupling parameter, a, deduced from the observed level energies [1] with that calculated with the single-particle wave function [11]. Rotational members up to spin 13/2 were identified in previous works. A γ-ray with 182.3-keV energy is tentatively assigned to the $15/2^+$ (420.0 keV) to $11/2^+$ transition.

A $3/2^+$ spin-parity for the 177.59-keV level is established from the $M1$ multipolarities of transitions to the $1/2^+$, $3/2^+$, and $5/2^+$ members of the ground-state band. This level was given $3/2^+[622]$ Nilsson-state assignment [12], and its rotational members up to $I = 11/2$ have been identified.

The decay pattern of the 106.30-keV level and multipolarities of transitions to the ground-state band fix the spin-parity of the level as $7/2^+$, and it was given a $7/2^+[613]$ assignment in Ref. [1]. Its rotational members up to $I = 15/2$ have been identified in the ^{255}Fm γ-ray spectrum. A 209.7-keV γ ray, observed in Fig. 2, could be the $17/2^+$ (535.0 keV) to $13/2^+$ transition. The spins and parities of the 105.74- and 106.30-keV levels were deduced from subshell conversion electron ratios [1]. In the present work, we have measured the intensities of γ rays deexciting these levels and thus have conversion coefficients that confirm the transition multipolarities.

The parity of the 543.98-keV level is determined to be positive on the basis of the measured $M1$ multipolarity of the

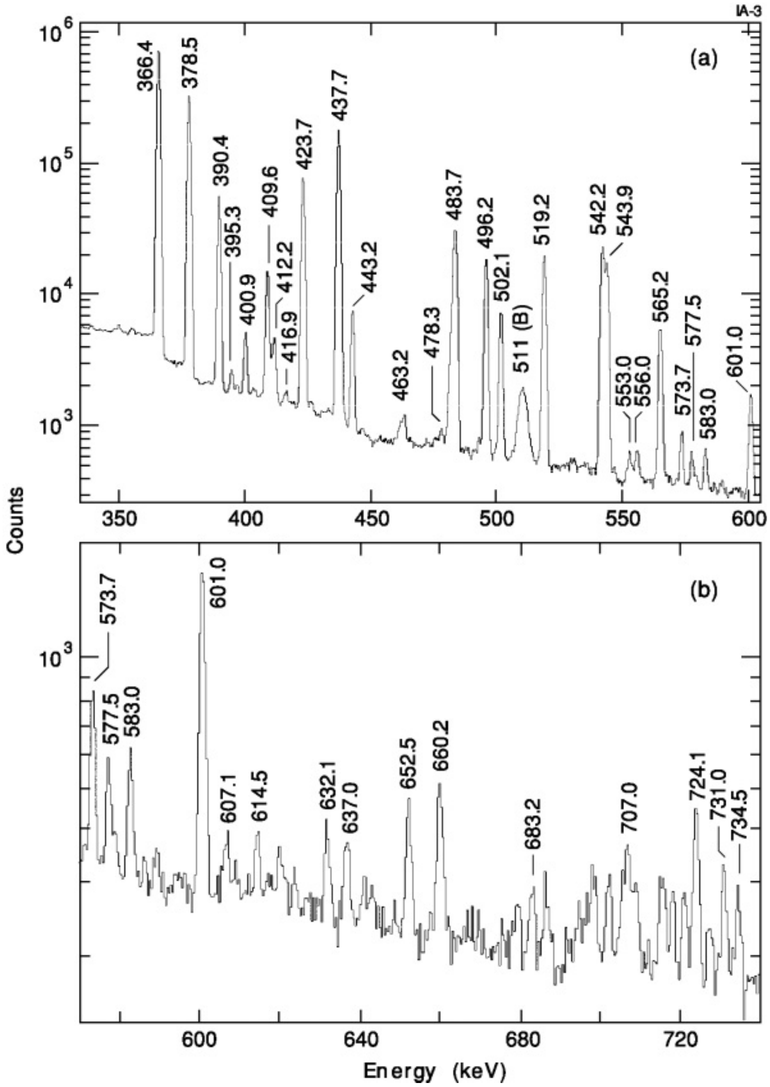

FIG. 3. ^{255}Fm γ-ray spectrum measured with a 25% Ge spectrometer, showing the ~340 to ~740 keV region. A set of Ta, Cd, Cu, and Fe absorbers was used to absorb low-energy γ rays, thus reducing the counting rate in the detector. The source was sandwiched between two 0.5-g/cm^2 Pt disks. The measurement was started 1 d after the chemical separation, and the counting time was 24 h.

366.4-keV transition deexciting this level to the $3/2^+$ level at 177.59 keV. The spin of this level is 5/2 because of its decay to the $1/2^+$ and $9/2^+$ members of the ground-state band. This band is assigned to the $5/2^+$[622] Nilsson-state [12] configuration.

The spin-parity of the 370.47-keV level is established as $11/2^-$ on the basis of its delayed decay to the members of the $7/2^+$ band and the $E1$ multipolarity of the 204.17-keV transition. In the same way the spin-parity of the 433.91-keV level is established as $9/2^-$ on the basis of its prompt decay to the $7/2^+$ band and the deduced multipolarity of the transition to the $11/2^-$ level. These states are given Nilsson-state configurations of $11/2^-$[725] and $9/2^-$[734], respectively.

The value of the K quantum number for a rotational band, which does not originate from a high-j orbital, can be determined from the measured energies of its rotational members and the rotational energy formula. We determine the K values of the bands at ground state, 106.30, 177.59, and 543.98 keV as 1/2, 7/2, 3/2, and 5/2, respectively, providing additional support for the above assignments. In Ref. [3], we showed that the cross sections measured for states in ^{251}Cf, populated in the ^{250}Cf(d, p) reaction, establish the single-particle characters of the above states as shown in the level scheme. A rotational band built on the 632.0-keV level was identified in the (d, p) reaction [3] and was given an assignment of $1/2^-$[750]. Gamma rays from this band were observed in the ^{255}Fm γ-singles spectrum and in the γ-γ coincidence spectrum measured with GAMMASPHERE [4], confirming the assignment made in the nuclear reaction studies.

In the ^{250}Cf(d, p) spectrum [3], a strong peak was observed at 972 keV. The decay γ rays from this level were identified in Ref. [4], and this level was given a single-particle assignment of $9/2^+$[604]. A more precise energy of 974.0 keV is obtained for this level from the γ-ray energies.

Spins of high-lying states observed in the present work have been deduced from their γ-ray decay pattern. Since transition multipolarities have not been determined, the parity of these states cannot be determined. α-decay hindrance factors, however, can be used for configuration assignments. It has been found that β- and octupole-vibrational bands in even-even nuclei have low hindrance factors. In odd-mass nuclei, vibrational bands built on the favored state have low hindrance factors. We have determined the α intensities to

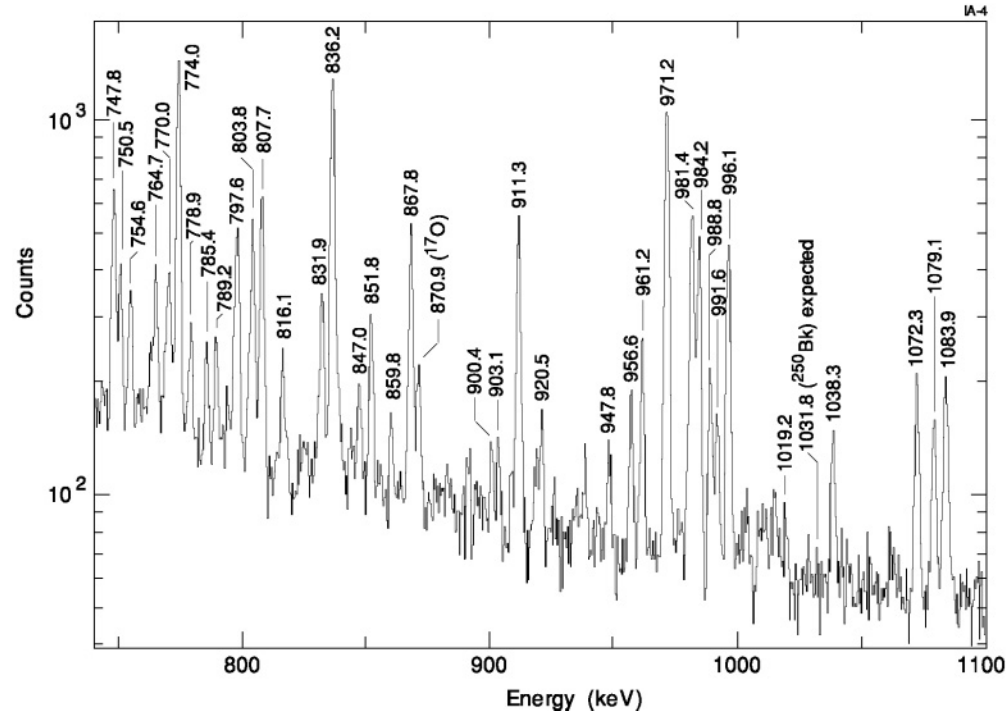

FIG. 4. Higher-energy portion of the ^{255}Fm γ-ray spectrum shown in Fig. 3. We did not detect any ^{250}Bk (^{254}Es daughter) γ line in this spectrum.

the high-lying states by adding the intensities of transitions deexciting these levels. Using these intensities, we calculated α-decay hindrance factors with the spin-independent theory of Preston [13]. The intensities of α groups and their hindrance factors are given in Table III. These are slightly different from the values given in Ref. [4] because, in the present work, we have identified more γ rays.

All levels above 900 keV (except the 974.0-keV level) shown in Fig. 7 are interpreted as vibrational states because of the low hindrance factors of the α transitions populating these states. Single-particle states with such low hindrance factors are not expected at these energies in ^{251}Cf. Energies of vibrational states in ^{251}Cf have not been calculated. However, energies of vibrational states with $K^\pi = 3/2^-, 5/2^-, 7/2^-$ in its isotone ^{249}Cm have been calculated by Gareev *et al.* [14]. They are compared with the energies of the proposed vibrational states later in this section. Because calculations are not available for the energies of vibrational states in ^{251}Cf and the parities of the levels have not been experimentally determined, the assignments of vibrational states in Fig. 7 are tentative.

The band built on the level at 981.4 keV was interpreted [4] as a vibrational band because of its low rotational constant, and the parity of the level was deduced as negative from its decay to the $1/2^-$ band at 632.0 keV. This band was interpreted [4] as a 2^- phonon built on the $7/2^+[613]$ band, with configuration $\{7/2^+[613] \otimes 2^-\}3/2^-$. The measured energy of 981.4 keV is in good agreement with the value of 910 keV calculated [14] in the isotone ^{249}Cm.

In the present work, because of the higher purity of the sample, we have been able to identify more γ rays, which has allowed us to propose more levels. A level at 1250.0 keV has been identified that has an α-decay hindrance factor of 23. This level decays to the $3/2^+$ band at 177.59 keV, to the $9/2^+$ level at 166.30 keV, and to the $9/2^-$ level at 433.91 keV, suggesting

TABLE III. ^{255}Fm α-decay hindrance factors calculated with the spin-independent theory of Preston [13], using a radius parameter of 9.400 fm. All α energies (except for the ground-state transition and the transition to the 106-keV level) were deduced from level excitation energies, and the intensity of each α group was obtained by adding intensities of transitions deexciting that level.

Excitation Energy (keV)	α Energy (keV)	Intensity (%)	Hindrance Factor
0.0	7127	0.07	4.4×10^3
106.3	7022	93.4	1.2
601	6535	$\sim4\times10^{-6}$	$\sim1.9\times10^5$
625	6512	$\sim4\times10^{-6}$	$\sim1.5\times10^5$
632	6505	$\sim3\times10^{-6}$	$\sim1.9\times10^5$
708	6430	$\sim6\times10^{-6}$	$\sim4.1\times10^4$
774	6365	3.8×10^{-5}	3.1×10^3
943	6199	3.6×10^{-5}	4.9×10^2
974	6168	2.3×10^{-5}	5.3×10^2
981	6161	4.1×10^{-5}	2.8×10^2
1009	6134	3.7×10^{-5}	2.2×10^2
1044	6099	2.2×10^{-5}	2.5×10^2
1078	6066	4.7×10^{-5}	77
1087	6057	1.0×10^{-5}	3.2×10^2
1095	6049	6.3×10^{-6}	4.7×10^2
1156	5989	$\sim4\times10^{-6}$	$\sim3.5\times10^2$
1185	5961	5.8×10^{-6}	1.7×10^2
1250	5897	1.9×10^{-5}	23

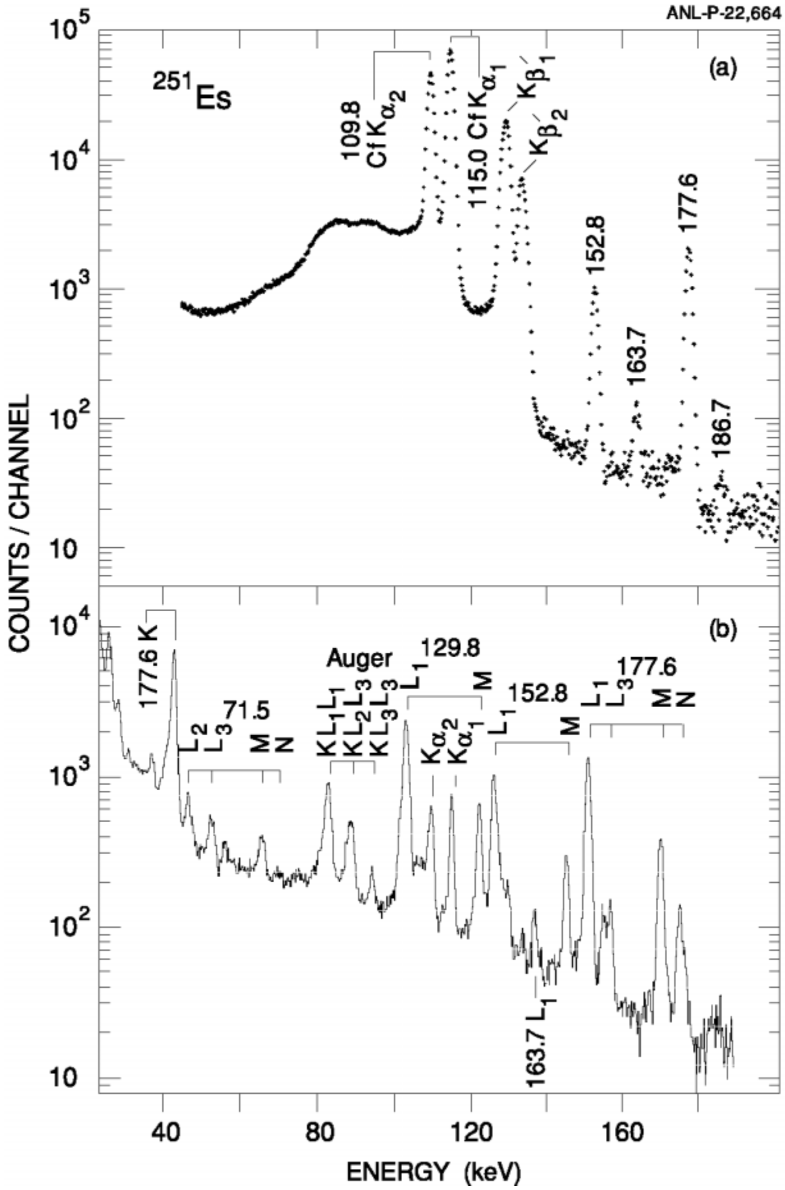

FIG. 5. Conversion electron spectrum of a mass-separated ^{251}Es source measured with a cooled Si(Li) electron spectrometer. Also shown is the corresonding ^{251}Es γ-ray spectrum measured with a 25-cm^3 Ge(Li) detector.

a possible spin-parity of $7/2^+$. This level has been assigned as $\{7/2^+[613] \otimes 0^+\}7/2^+$ because of the low α-decay hindrance factor.

In Ref. [4], the 1077.5-keV level was shown to decay by 971.2- and 911.3-keV strong transitions to the $7/2^+[613]$ band, and the only possible spin values were 7/2 and 9/2. This level was given a tentative assignment of $\{7/2^+[613] \otimes 0^+\}7/2^+$ because of the low α-decay hindrance factor. In the present work, because of higher sensitivity we have identified three weak γ rays with energies 643.6, 707.0, and 838.4 keV and assigned them to the decay of the 1077.5-keV level. An 838.5 ± 0.3 keV γ ray was identified in ^{253}Es α decay [15] with about the same intensity as that of the 838.4 ± 0.3 keV γ ray in ^{255}Fm decay. The appearance of the same γ ray in the spectra of two different nuclides suggests that it might be from a contaminant, most likely a fission product. However, we have not been able to assign it to any known nuclide and hence have left it assigned to ^{255}Fm α decay. The decay of the 1077.5-keV level, shown in Fig. 7, indicates $K, I = 9/2,9/2$ for this level, which is different from the assignment of $K, I = 7/2,7/2$ made in Ref. [4]. No single-particle or vibrational state with such a low α-decay hindrance factor is expected in this energy region. This state is most likely a three-quasiparticle state.

Gamma-ray transitions indicate a level at 1086.5 keV. This level decays to the 9/2 and 11/2 members of the $7/2^+[613]$ band, to the $9/2^-$ level at 433.91 keV, and to the $11/2^-$ level at 370.47 keV. This decay pattern indicates $9/2^-$ spin-parity for this level. This level has been assigned as the $\{7/2^+[613] \otimes 1^-\}9/2^-$ vibrational state.

We have made a tentative identification of a level at 1185.5 keV, which decays to the $7/2^+$ level at 106.30 keV, $9/2^+$ level at 166.30 keV, and $5/2^+$ level at 543.98 keV. Possible spin values for this level are 5/2 or 7/2. We have made no configuration assignment for this level.

In Ref. [4] and in spectra measured in the present work, three strong γ rays with energies of 774.0, 836.2, and

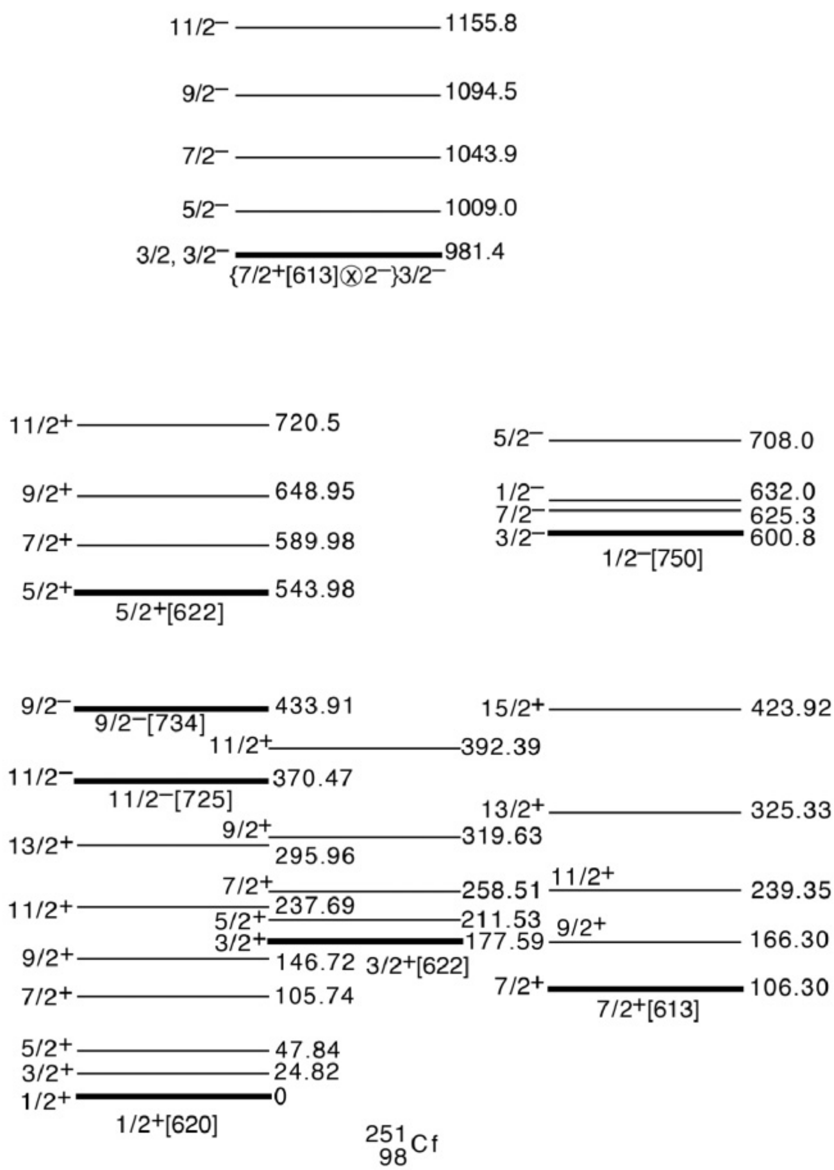

FIG. 6. Low-energy levels of ^{251}Cf deduced from previous studies. Level energies in kiloelectron volts are from the present work. The Nilsson-state configuration is shown below each band. The $K^{\pi} = 3/2^-$ band at 981.4 keV is assigned to the $\{7/2^+[613] \otimes 2^-\}3/2^-$ configuration.

870.9 keV have been identified in the ^{255}Fm γ-ray spectrum, which could not be placed in the level scheme. The intensity of the 870.9-keV γ ray was reduced when the source was sandwiched between two Pt disks, indicating that this γ ray does not belong to ^{255}Fm α decay and that it is produced in the ^{14}N(α, $p\gamma$) reaction. The 774.0- and 836.2-keV γ rays have roughly the same intensities relative to those of known ^{255}Fm γ rays in all spectra and decay with roughly the same half-life as ^{255}Fm. These observations suggest that these two γ rays belong to the ^{255}Fm decay. The 836.2-keV γ ray has been tentatively assigned to the decay of a 942.5-keV level. This level also decays to the $3/2^+[622]$ band at 177.59 keV, as indicated by the coincidence of the 731.0- and 764.7-keV γ rays with Cf K x rays. The most likely spin-parity for this level is $5/2^-$, and we assign this level as a $\{7/2^+[613] \otimes 1^-\}5/2^-$ configuration. The energy of this state is calculated [14] in the isotone ^{249}Cm to be 1160 keV, which is moderately higher than the experimental energy.

In Ref. [3] a very small peak was observed in the ^{250}Cf(d, p) reaction at an excitation energy of 775 keV. The small cross section indicates that it is a hole state. We tentatively assign this state to the 3/2 member of the $1/2^+[631]$ Nilsson state and the 774.0-keV γ ray as the transition from this level to the ground state of ^{251}Cf. However, we have not identified any other transition from the decay of the $1/2^+[631]$ band.

There are several γ rays that could not be placed in the level scheme, and these are given at the end of Table I. These γ rays could belong to the $1/2^+[631]$ and $7/2^+[624]$ Nilsson orbitals, which are expected to lie below 1 MeV excitation in ^{251}Cf. We have not observed any γ ray from the decay of the $9/2^+[615]$ Nilsson state, which was identified at 683 keV in the (d, p) reaction [3].

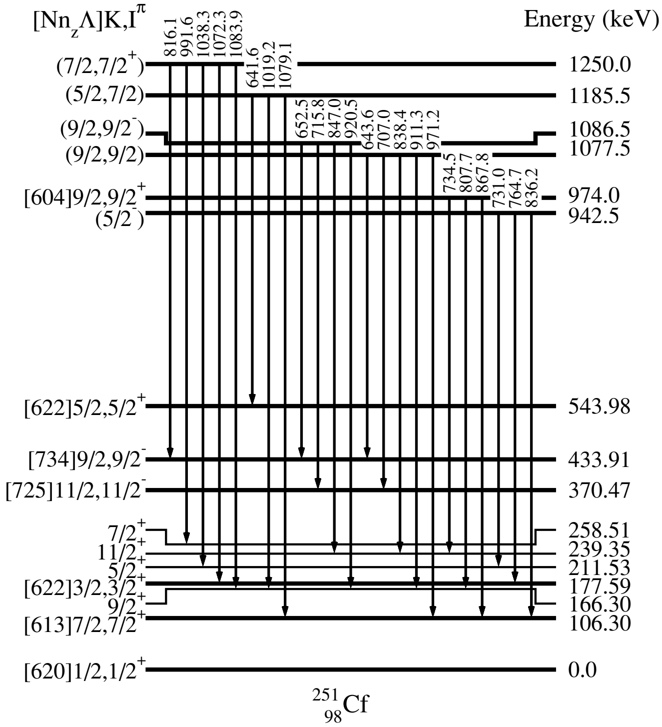

FIG. 7. New vibrational levels in ^{251}Cf identified in the present work. The states at 942.5, 1086.5, and 1250.0 keV are vibrational states with configurations $\{7/2^+[613] \otimes 1^-\}5/2^-$, $\{7/2^+[613] \otimes 1^-\}9/2^-$, and $\{7/2^+[613] \otimes 0^+\}7/2^+$, respectively. The 1185.5-keV level has a likely spin of 5/2 or 7/2, and the 1077.5-keV level is given spin assignment of 9/2. Single-particle states were identified in previous studies.

The experimental energies of single-particle states in ^{251}Cf have been compared with values calculated with a Woods-Saxon potential in Ref. [4]. The calculated level orderings and spacings were found to be in excellent agreement with the orderings and spacings extracted from the experimental data.

B. *g*-factor measurement

Several members of the $7/2^+[613]$ band have been identified in the present work. Using the measured cascade to cross over γ-ray branching ratios and a quadrupole moment of $Q = 12.9$ eb [16], we have deduced the $|g_K - g_R|$ values. The average value of $|g_K - g_R|$ for the $7/2^+[613]$ band is $|g_K - g_R| = 0.66 \pm 0.05$. This is in excellent agreement with the theoretical value of $|g_K - g_R| = 0.64$ for the $7/2^+[613]$ orbital calculated with the single-particle wavefunctions of Ref. [11] using a g_R value of $g_R = 0.31$.

C. Summary

Gamma-ray spectra of pure ^{255}Fm sources and the electron spectrum of a mass-separated ^{251}Es source have been measured with high-resolution spectrometers. These measurements confirm the assignments of single-particle and vibrational states identified in previous decay studies and (d, p) reaction spectroscopic measurements. These include 1/2+[620], 0.0 keV; $7/2^+[613]$, 106.30 keV; $3/2^+[622]$, 177.59 keV; $11/2^-[725]$, 370.47 keV; $9/2^-[734]$, 433.91 keV; $5/2^+[622]$, 643.98 keV; $1/2^-[750]$, 632.0 keV; $9/2^+[615]$, 683 keV; $9/2^+[604]$, 974.0 keV; and $\{7/2^+[613] \otimes 2^-\}3/2^-$, 981.4 keV. Three new states are identified in the present work at 942.5, 1086.5, and 1250.0 keV. These are given tentative assignments of $\{7/2^+[613] \otimes 1^-\}5/2^-$, $\{7/2^+[613] \otimes 1^-\}9/2^-$, and $\{7/2^+[613] \otimes 0^+\}7/2^+$, respectively. A level was identified at 1185.5 keV that decays to the $7/2^+$ level at 106.30 keV, $9/2^+$ level at 166.30 keV, and $5/2^+$ level at 543.98 keV, suggesting a spin of 5/2 or 7/2. A level was identified at 1077.5 keV, and its decay pattern suggests a spin value of 9/2. The energies of the vibrational states in ^{251}Cf are very similar to the energies of corresponding vibrational states in ^{250}Cf [17,18] and ^{249}Bk [15] and are in good agreement with the values calculated by Gareev *et al.* [14] for vibrational states in the isotone ^{249}Cm.

ACKNOWLEDGMENTS

The authors acknowledge helpful discussions with J. Knauer and the assistance of R. D. Vandergrift and F. D. Riley in the isolation and purification of ^{255}Fm samples. The authors are also indebted for the use of ^{255}Fm to the Office of Basic Energy Sciences, U.S. Department of Energy, through the transplutonium element production facilities at Oak Ridge National Laboratory. This work was supported by the U.S. Department of Energy, Office of Nuclear Physics, under contract W-31-109-ENG-38 (ANL) and Department of Energy, Office of Basic Energy Sciences, under contract DE-AC05-00OR22725 (ORNL).

[1] I. Ahmad, F. T. Porter, M. S. Freedman, R. F. Barnes, R. K. Sjoblom, F. Wagner, Jr., J. Milsted, and P. R. Fields, Phys. Rev. C **1**, 390 (1971).

[2] I. Ahmad and J. Milsted, Nucl. Phys. **A239**, 1 (1975).

[3] I. Ahmad, R. R. Chasman, A. M. Friedman, and S. W. Yates, Phys. Lett. **B251**, 338 (1990).

[4] I. Ahmad, M. P. Carpenter, R. R. Chasman, J. P. Greene, R. V. F. Janssens, T. L. Khoo, F. G. Kondev, T. Lauritsen, C. J. Lister, P. Reiter, D. Seweryniak, A. Sonzogni, J. Uusitalo, I. Wiedenhöver, and P. Bhattacharyya, Phys. Rev. C **62**, 064302 (2000).

[5] I. Ahmad, R. K. Sjoblom, R. F. Barnes, E. P. Horwitz, and P. R. Fields, Nucl. Phys. **A140**, 141 (1970).

[6] E. Browne and R. B. Firestone, *Table of Radioactive Isotopes* (Wiley, New York, 1986).

[7] T. R. England and B. F. Rider, Los Alamos National Laboratory Reports LA-UR-94-3106; ENDF-349, 1993 (unpublished).

[8] I. Ahmad, R. K. Sjoblom, A. M. Friedman, and S. W. Yates, Phys. Rev. C **17**, 2163 (1978).
[9] I. M. Band, M. B. Trzhaskovskaya, C. W. Nestor Jr., P. O. Tikkanen, and S. Raman, At. Data Nucl. Data Tables **81**, 1 (2002).
[10] I. Ahmad, R. R. Chasman, J. P. Greene, F. G. Kondev, E. F. Moore, E. Browne, C. E. Porter, and L. K. Felker, Phys. Rev. C **68**, 044306 (2003).
[11] R. R. Chasman, I. Ahmad, A. M. Friedman, and J. R. Erskine, Rev. Mod. Phys. **49**, 833 (1977).
[12] S. G. Nilsson, Mat. Fys. Medd. K. Dan. Vidensk. Selsk. **29**, 16 (1955).
[13] M. A. Preston, Phys. Rev. **71**, 865 (1947).
[14] F. A. Gareev, S. P. Ivanova, L. A. Malov, and V. G. Soloviev, Nucl. Phys. **A171**, 134 (1971).
[15] I. Ahmad, F. G. Kondev, E. F. Moore, M. P. Carpenter, R. R. Chasman, J. P. Greene, R. V. F. Janssens, T. Lauritsen, C. J. Lister, D. Seweryniak, R. W. Hoff, J. E. Evans, R. W. Lougheed, C. E. Porter, and L. K. Felker, Phys. Rev. C **71**, 054305 (2005).
[16] J. L. Ford Jr., P. H. Stelson, C. E. Bemis Jr., F. K. McGowan, R. L. Robinson, and W. T. Milner, Phys. Rev. Lett. **27**, 1232 (1971).
[17] I. Ahmad, A. M. Friedman, and S. W. Yates, Phys. Rev. C **21**, 874 (1980).
[18] I. Ahmad and R. K. Sjoblom, Phys. Rev. C **22**, 1226 (1980).